Available online at www.sciencedirect.com
ScienceDirect
Journal of Power Sources 179 (2008) 96–100
JOURNAL OF POWER SOURCES
www.elsevier.com/locate/jpowsour

Short communication

La substituted Sr_2MnO_4 as a possible cathode material in SOFC

Sun Liping [a], Huo Lihua [a], Zhao Hui [a,*], Li Qiang [a], Christophe Pijolat [b]

[a] *Laboratory of Functional Materials, School of Chemistry and Materials Science, Heilongjiang University, Harbin 150080, China*
[b] *Ecole Nationale Supérieure des Mines, Centre SPIN, LPMG-URA CNRS 2021, Saint Etienne Cedex 2, France*

Received 26 October 2007; received in revised form 15 December 2007; accepted 18 December 2007
Available online 4 January 2008

Abstract

$Sr_{2-x}La_xMnO_{4+\delta}$ ($x = 0.4$, 0.5, 0.6) oxides were studied as the cathode material for solid oxide fuel cells (SOFC). The reactivity tests indicated that no reaction occurred between $Sr_{2-x}La_xMnO_{4+\delta}$ and CGO at annealing temperature of 1000 °C, and the electrode formed good contact with the electrolyte after being sintered at 1000 °C for 4 h. The total electrical conductivity, which has strong effect on the electrode properties, was determined in a temperature range from 100 to 800 °C. The maximum value of 5.7 S cm^{-1} was found for the $x = 0.6$ phase at 800 °C in air. The cathode polarization and AC impedance results showed that $Sr_{1.4}La_{0.6}MnO_{4+\delta}$ exhibited the lowest cathode overpotential. The area specific resistance (ASR) was 0.39 Ω cm^2 at 800 °C in air. The charge transfer process is the rate-limiting step for oxygen reduction reaction on $Sr_{1.4}La_{0.6}MnO_{4+\delta}$ electrode.

Keywords: Solid oxide fuel cell (SOFC); $Sr_{2-x}La_xMnO_{4+\delta}$ cathode material; Electrode reaction

1. Introduction

To realize low cost intermediate temperature solid oxide fuel cells (IT-SOFCs), the operating temperature must be reduced to 800 °C or lower. An issue of significant importance for the development of IT-SOFC is the selection of an appropriate cathode material.

Up to now, most of the studies concerned with cathode materials for IT-SOFC are devoted to perovskite-type oxides, such as LSCF. It was reported that $La_{1-\alpha}Sr_\alpha Co_{1-\beta}Fe_\beta O_{3-\delta}$ has unacceptably high thermal expansion coefficient for $0.4 < \alpha < 1$ and $0.5 < \beta < 1$ [1,2]. A_2MO_4 oxides with the K_2NiF_4-type structure, which can accommodate large amount of oxygen non-stoichiometry, have much higher thermochemical stability compared to the related AMO_3-type materials [3]. Preliminary results are promising in terms of oxygen diffusion and thermal expansion coefficient [4,5]. The majority of these investigations have concentrated on the suitability of Cu, Ni, Fe and Co substituted materials due to their excellent electrode performance [6–10]. Munnings et al. prepared $Sr_{2-x}La_xMnO_{4+\delta}$ and studied their structure, stability and electrical conductivity. The investigation indicated that $Sr_{2-x}La_xMnO_{4+\delta}$ has good thermochemical stability over a wide range of oxygen partial pressures and the thermal expansion coefficient is also comparable to the most commonly available electrolyte materials [11]. This would lead to interesting engineering possibilities in terms of developing cathode structures. In this work, $Sr_{2-x}La_xMnO_{4+\delta}$ ($x = 0.4$, 0.5, 0.6) materials were synthesized through glycine-nitrate process and their electrocatalyst properties were investigated systematically in relation to the requirement of SOFC cathode.

2. Experimental

$Sr_{2-x}La_xMnO_{4+\delta}$ powders were synthesized using the glycine-nitrate process (GNP). According to the formula $Sr_{2-x}La_xMnO_{4+\delta}$ ($x = 0.4$, 0.5, 0.6), stoichiometric amount of $La(NO_3)_3$, $Sr(NO_3)_2$ and $Mn(NO_3)_2$ solutions were mixed in a beaker, to which glycine (aminoacetic acid, $H_2NCH_2CO_2H$) was added at 1:2 molar ratios of metal ions/glycine. After drying and firing, the resultant powders were calcined in air at 1373 K for 12 h. $Ce_{0.9}Gd_{0.1}O_{1.9}$ (CGO) powders were prepared according to ref. [12]. CGO powders were pressed uniaxially at 220 MPa and then sintered at 1400 °C for 10 h to form a densified pellet. The $Sr_{2-x}La_xMnO_{4+\delta}$ powders were mixed with terpineol to form a slurry, and subsequently painted on one side of the CGO electrolyte to form an electrode area of 1.0 cm^2,

* Corresponding author. Tel.: +86 45186608040; fax: +86 45186608040.
E-mail address: zhaohui98@yahoo.com (Z. Hui).

0378-7753/$ – see front matter © 2007 Elsevier B.V. All rights reserved.
doi:10.1016/j.jpowsour.2007.12.090

used as working electrode (WE). Platinum paste was painted on the other side of the CGO pellet in symmetric configuration, as the counter electrode (CE). A Pt wire was used as reference electrode (RE) and painted on the same side that of the working electrode. The cathode was first heated at 400 °C for 2 h to eliminate organic binders, followed by sintering at 1000 °C for 4 h in air, with a heating/cooling rate of 3 °C min^{-1}. The sample was characterized using X-ray diffraction (XRD) (Rigaku, D/MAX-3B) and scanning electron microscopy (SEM) (Hitachi, S-4700 FEG), respectively. The electrical conductivity of the $Sr_{2-x}La_xMnO_{4+\delta}$ materials was measured by the standard four-probe DC method. Rods of $Sr_{2-x}La_xMnO_{4+\delta}$ were sintered at 1350 °C for 6 h in air. The density of the sintered rods was measured by Archimedes method. The relative density of specimens ranged from 85% to 91%. Rectangular bars with dimension of 5 mm × 5 mm × 20 mm were obtained from the sintered rods. Pt lead was attached to the rectangular bar with Pt paste and fired at 800 °C for 1 h to obtain good electric contact. Measurements were performed from room temperature to 800 °C with a heating rate of 5 °C min^{-1}. AC impedance spectroscopy was done using Autolab PGStat30 (Holland) in the frequency range of 0.1 Hz–1 MHz at temperatures between 600 and 800 °C. Oxygen partial pressure was varied between 1.0×10^{-3} and 1.0 atm using O_2/N_2 gas mixtures.

3. Results and discussions

The powder XRD patterns are plotted in Fig. 1. Only three compositions of $Sr_{2-x}La_xMnO_{4+\delta}$ ($x = 0.4$, 0.5, 0.6) were obtained as single phases by heating the precursors at 1100 °C in air for 12 h (Fig. 1(a)). The other compositions with $x < 0.4$ and/or $x > 0.6$ cannot be prepared as pure phases in air. The similar conclusion has been made before by Munnings et al. when they prepared $Sr_{2-x}La_xMnO_{4+\delta}$ by solid-state reaction [11]. The XRD patterns of $Sr_{2-x}La_xMnO_{4+\delta}$ were indexed on a body-centered tetragonal unit cell, consistent with a structure related to K_2NiF_4. Fig. 1(b) shows the XRD patterns of mixtures of $Sr_{2-x}La_xMnO_{4+\delta}$ and CGO powders after heat-treated at 1000 °C for 12 h. Obviously the CGO and $Sr_{2-x}La_xMnO_{4+\delta}$ remained their structures unchanged. There are no new peaks identifiable in the patterns, indicating that there is no reaction between $Sr_{2-x}La_xMnO_{4+\delta}$ and CGO.

Arrehnius plots for the electrical conductivity of $Sr_{2-x}La_xMnO_{4+\delta}$ ($x = 0.4$, 0.5, 0.6) are given in Fig. 2. The conductivities, σ, were measured in the temperature range 100–800 °C in air. The electrical conductivity of the $Sr_{2-x}La_xMnO_{4+\delta}$ oxides increased with temperature, indicating thermally activated semiconductivity. The highest electrical conductivity was obtained for $x = 0.6$ and the value is about 5.7 S cm^{-1}. The activation energy of conduction was determined from the plot, using the following expression derived for the small polaron mechanism:

$$\sigma = \frac{A}{T} \exp\left(\frac{-E_a}{\kappa T}\right)$$

where A is the pre-exponential factor, κ is the Boltzmann constant, T is the absolute temperature and E_a is the activation energy. It can be seen from Fig. 2 that the electrical conductivities obtained in this work were similar with those reported by Skinner and coworkers [11] and Daroukh et al. [13], especially at high temperature. But the activation energies are relatively

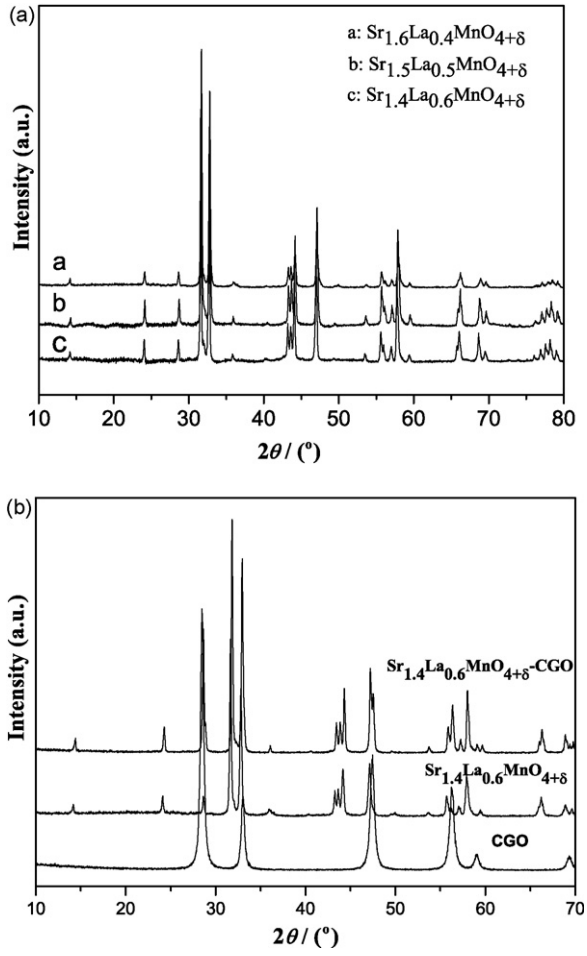

Fig. 1. The XRD patterns of (a) $Sr_{2-x}La_xMnO_{4+\delta}$ as synthesized and (b) $La_{0.6}Sr_{1.4}MnO_{4+\delta}$ +CGO after heat-treatment at 1000 °C for 12 h.

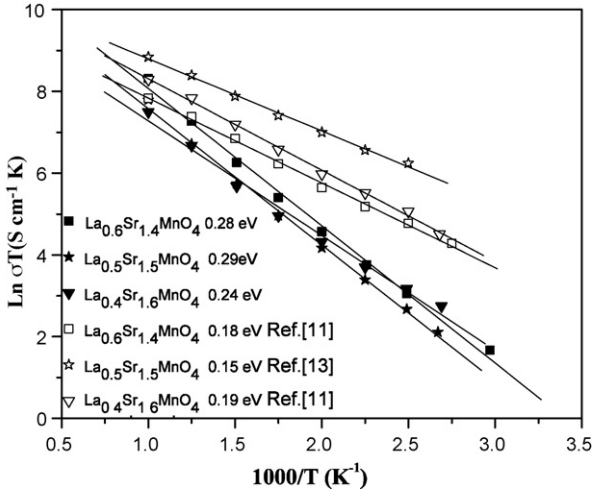

Fig. 2. Temperature dependence of the electrical conductivity for $La_{2-x}Sr_xMnO_{4+\delta}$ ($x = 1.4$, 1.5, 1.6).

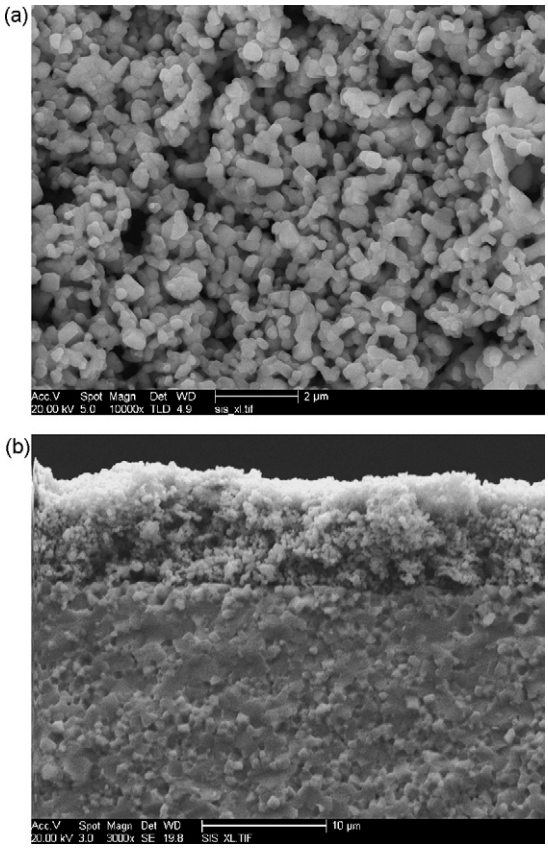

Fig. 3. Surface (a) and cross-sectional micrographs (b) of $La_{0.6}Sr_{1.4}MnO_{4+\delta}$ electrode on CGO electrolyte.

higher than the reported values. The possible reason may come from the different preparation methods of these oxides.

The microstructure of $La_{0.6}Sr_{1.4}MnO_{4+\delta}$/CGO test cell was given in Fig. 3. The $La_{0.6}Sr_{1.4}MnO_{4+\delta}$ electrode sintered at 1000 °C for 4 h shows a structure with reasonable porosity and well-necked particles. The good adhesion between electrode and electrolyte is also observed. The average particle and pore sizes were in the range of 200–300 nm and the thickness of the cathode layer was about 10 μm, respectively.

Fig. 4 shows the typical Nyquist plots vs. temperature for $La_{0.6}Sr_{1.4}MnO_{4+\delta}$ cathode. The intercept value of the impedance arcs with the real axis at high frequency side corresponds to the resistance of the electrolyte and lead wires, while the value between the high frequency x-axis intercept and the low frequency one is attributed to the total polarization resistance (R_p) of $La_{0.6}Sr_{1.4}MnO_{4+\delta}$ electrode. The electrode area specific resistance (ASR) was calculated by multiplying the total polarization resistance with the electrode area. As expected, the electrode ASR increased with the decrease of temperature, showing that the electrode activity changes monotonously with the temperature. At low temperature, significant overlap was observed between the high- and low-frequency arcs, giving the appearance of a single pressed arc. At 800 °C, however, we can obviously observed two arcs.

The temperature dependence of polarization resistance for $La_{2-x}Sr_xMnO_{4+\delta}$ (x = 1.4, 1.5, 1.6) materials is shown in Fig. 5. The polarization resistance reduced with the decrease of Sr-

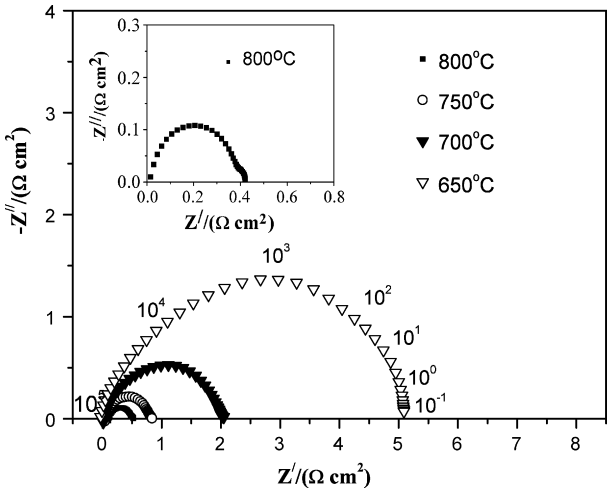

Fig. 4. Impedance spectra taken from $La_{0.6}Sr_{1.4}MnO_{4+\delta}$ cathodes in air at various temperatures. (The electrolyte resistance was deduced in the Nyquist plot).

doping content over the entire examined temperature range. The lowest ASR was obtained when the value of x reached 1.4. From the Arrhenius plot of the electrode ASR, the activation energy can be calculated. The values are around 1.39–1.55 eV for all the samples studied. These values are quite similar to the reported activation energy of the oxygen surface exchange process that occurred on $La_2NiO_{4+\delta}$ and $La_{1.9}Sr_{0.1}NiO_{4+\delta}$ electrode [14]. Considering the structural similarity of $La_{0.6}Sr_{1.4}MnO_{4+\delta}$ and $La_2NiO_{4+\delta}$, we proposed that the oxygen reduction reaction on $La_{0.6}Sr_{1.4}MnO_{4+\delta}$ electrode was mainly determined by the oxygen surface exchange process.

In order to further understand the oxygen reduction mechanism on the electrodes, impedance measurements were done as a function of oxygen partial pressure. Fig. 6 shows the impedance spectra of $La_{0.6}Sr_{1.4}MnO_{4+\delta}$ cathode at 800 °C under various oxygen partial pressures (P_{O_2}). Two impedance arcs are observed at low and high frequencies side, which indicates that the oxygen reduction reaction was limited at least by two electrode processes. In order to separate the different contributions,

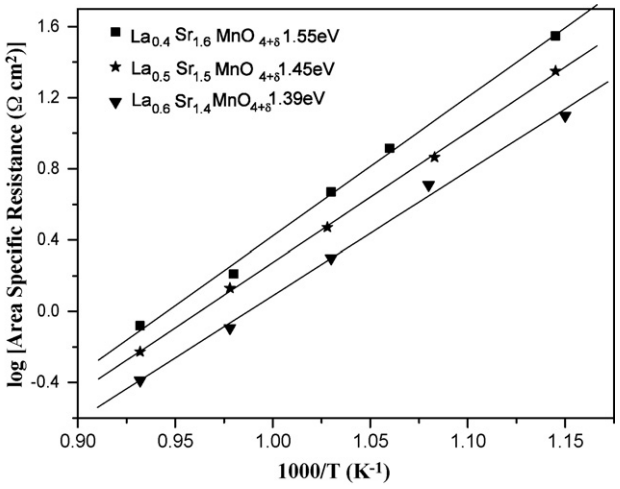

Fig. 5. Arrhenius plots of the polarization resistances of $La_{2-x}Sr_xMnO_{4+\delta}$ (x = 1.4, 1.5, 1.6) electrodes under air.

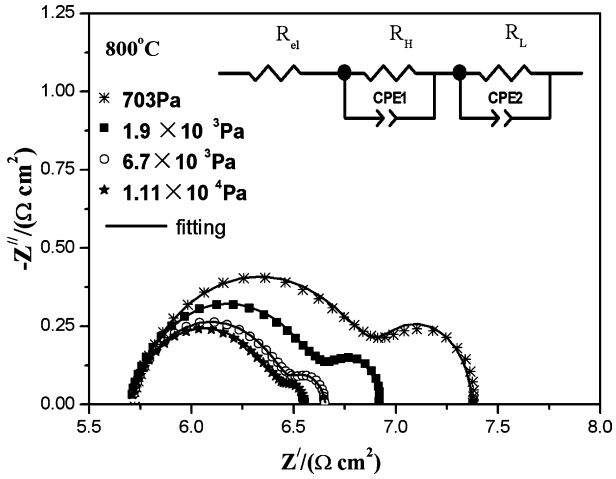

Fig. 6. Impedance spectra for the $La_{0.6}Sr_{1.4}MnO_{4+\delta}$ cathode on CGO at 800 °C under various oxygen partial pressures.

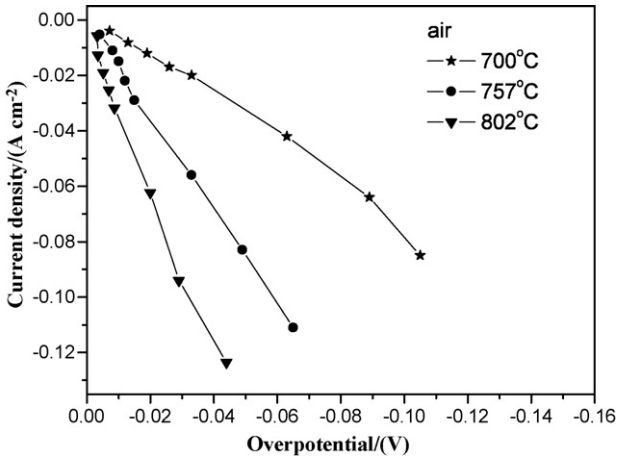

Fig. 8. The overpotential-current density curves measured in air at various temperatures.

an equivalent circuit with two distributed elements was used to fit the data. As shown in Fig. 6, R_{el} is the combination of electrolyte resistance, electrode ohmic resistance, lead resistance and contact resistance between cell and Pt mesh, CPE is the constant phase element in parallel with a resistance (R), R_H and R_L are the resistance corresponding to the high-frequency and low-frequency arc, respectively. It was found that R_{el} remains unchanged with the change of oxygen partial pressure. The electrode polarization resistances of $La_{0.6}Sr_{1.4}MnO_{4+\delta}$ at 800 °C under various P_{O_2} are shown in Fig. 7, from which the P_{O_2} dependence of the ASR can be calculated.

Generally, ASR of the electrode varies with the oxygen partial pressure according to the following equation [15,16]

$$[\mathrm{ASR}] = [\mathrm{ASR}]_0 (P_{O_2})^{-m}$$

The magnitude of m provides an insight into the rate-limiting step of the oxygen reduction reaction on the electrodes. For metal and metal oxide electrodes on solid electrolytes, $m = 0.25$ has been attributed to the charge-transfer reaction at the triple-phase boundary, $m = 0.5$ to the surface diffusion of the dissociative adsorbed oxygen at the triple-phase boundaries (TPBs), and $m = 1$ to gaseous diffusion of oxygen molecules in the porous structure. As can be seen from Fig. 7, the polarization resistance of high-frequency arc is larger than that of low-frequency arc. A 0.55–0.65 P_{O_2} dependency of R_L was observed. Considering that this value locates between 0.5 and 1, we suggest this process relate to a mixed control mechanism, both including the surface diffusion of the dissociative adsorbed oxygen at the triple-phase boundaries, and the gas phase diffusion phenomena. The characteristic of R_H of $La_{0.6}Sr_{1.4}MnO_{4+\delta}$ in this study showed 0.25 P_{O_2} dependency, which could be related to the charge-transfer reaction at the triple-phase boundary. So in this study, the charge-transfer reaction becomes the major rate-limiting step in the whole range of measurement oxygen partial pressure.

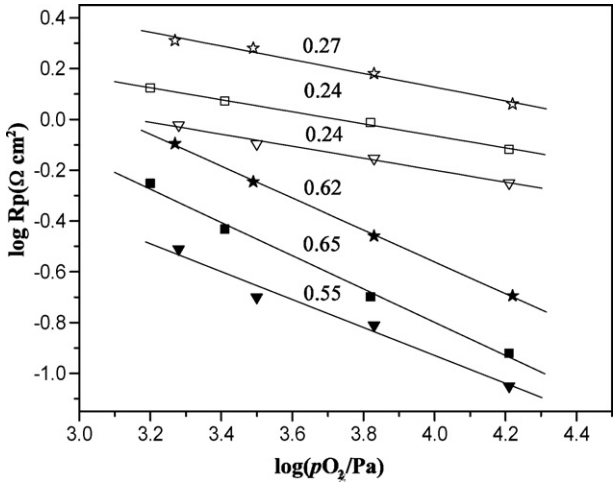

Fig. 7. Polarization resistance of $La_{0.6}Sr_{1.4}MnO_{4+\delta}$ electrode vs. P_{O_2} at various temperatures. (■, R_L 750 °C; ▼, R_L 800 °C; ★, R_L 700 °C; □, R_H 750 °C; ▽, R_H 800 °C; ☆, R_H 700 °C).

Cathode overpotential is an important factor representing the electrode performance. Fig. 8 showed the dc polarization curves measured at different temperatures in air. It was observed that the current density increases with increasing temperatures. The lowest polarization overpotential, 44 mV was obtained for $La_{0.6}Sr_{1.4}MnO_{4+\delta}$ cathode at a current density of 123 mA cm^{-2} at 800 °C in air. This value is better than that of the reported $Sm_{2-x}Sr_xNiO_4$ materials in literature [8]. Here, we should note that the total conductivity of $La_{0.6}Sr_{1.4}MnO_{4+\delta}$ is quite low compared to $La_2NiO_{4+\delta}$ [17] and LSCF [18]. It seems that the use of this material as SOFC cathode would be limited. However, we found that the polarization resistance of this material is much lower than the reported $La_{2-x}Sr_xNiO_4$ [19]. We propose the improved oxygen exchange and diffusion properties of $La_{0.6}Sr_{1.4}MnO_{4+\delta}$ material would play a critical role in the oxygen reduction reaction, as that observed before for LSCF material [20]. Further study is needed to investigate the oxygen ions transfer properties of $La_{2-x}Sr_xMnO_{4+\delta}$ material.

4. Conclusions

$Sr_{2-x}La_xMnO_{4+\delta}$ ($x = 0.4$, 0.5, 0.6) materials have been investigated as prospective cathode for IT-SOFC based on ceria

electrolytes. No reaction was found between $La_{0.6}Sr_{1.4}MnO_{4+\delta}$ electrode and CGO electrolyte after heat-treatment at 1000 °C for 12 h, indicated high chemical compatibility of these materials at high temperature. The reaction rate-limiting step for oxygen reduction on the electrode is the charge transfer process. The lowest R_p value was achieved for $La_{0.6}Sr_{1.4}MnO_{4+\delta}$ ($0.39\,\Omega\,cm^2$) at 800 °C and the highest current density is $123\,mA\,cm^{-2}$ at overpotential of 44 mV. The $Sr_{2-x}La_xMnO_{4+\delta}$ materials can be used as new cathode materials for SOFC.

Acknowledgements

The Project was supported by Science Foundation for Distinguished Young Scholars of Heilongjiang Province and Key Project of Chinese Ministry of Education (206044, 205050).

References

[1] A. Petric, R. Peng Huang, F. Tietz, Solid State Ionics 135 (2000) 719–725.
[2] H. Ullmann, N. Trofimenko, F. Tietz, D. Stőver, A. Ahmad-Khanlou, Solid State Ionics 138 (2000) 79–90.
[3] V.V. Kharton, A.A. Yaremchenko, A.L. Shaula, M.V. Patrakeev, E.N. Naumovich, D.I. Logvinovich, J.R. Frade, F.M.B. Marques, J. Power Sources 177 (2004) 26–37.
[4] L. Minervini, R. Grimes, J. Kilner, K. Sickafus, J. Mater. Chem. 10 (2000) 2349–2354.
[5] V. Vashook, I. Yushkevich, L.V. Kokhanovsky, L.V. Makhnach, S. Tolochko, I.F. Kononyuk, H. Ullmann, H. Altenburg, Solid State Ionics 119 (1999) 23–30.
[6] D.M. Bochkov, V.V. Kharton, A.V. Kovalevsky, A.P. Viskup, E.N. Naumovich, Solid State Ionics 120 (1999) 281–288.
[7] V.V. Kharton, A.P. Viskup, A.V. Kovalevsky, E.N. Naumovich, F.M.B. Marques, Solid State Ionics 143 (2001) 337–353.
[8] Q. Li, Y. Fan, H. Zhao, L.P. Sun, L.H. Huo, J. Power Sources 167 (2007) 64–68.
[9] A.J. Jennings, S.J. Skinner, Solid State Ionics 152–153 (2002) 663–667.
[10] Q. Li, H. Zhao, L.H. Huo, L.P. Sun, X.L. Cheng, J.C. Grenier, Electrochem. Commun. (9) (2007) 1508–1512.
[11] C.N. Munnings, S.J. Skinner, G. Amow, P.S. Whitfield, I.J. Davidson, Solid State Ionics 177 (2006) 1849–1853.
[12] S. Zha, A. Moore, H. Abernathy, M. Liu, J. Electrochem. Soc. 151 (8) (2004) A1128–A1133.
[13] M.A. Daroukh, V.V. Vashook, H. Ullmann, F. Tietz, I.A. Raj, Solid State Ionics 158 (2003) 141–150.
[14] S.J. Skinner, J.A. Kilner, Solid State Ionics 135 (2000) 709–712.
[15] E. Sicbeit, A. Hammouche, M. Kleitz, Electrochim. Acta 40 (1995) 1741–1753.
[16] J.D. Kim, G.D. Kim, J.W. Moon, Y. Park, W.H. Lee, K. Kobayashi, M. Nagai, C.E. Kim, Solid State Ionics 143 (2001) 379–389.
[17] D.P. Huang, Q. Xu, F. Zhang, W. Chen, H.X. Liu, J. Zhou, Mater. Lett. 60 (2006) 1892–1895.
[18] A. Mineshige, J. Izutsu, M. Nakamura, K. Nigaki, J. Abe, M. Kobune, S. Fujii, T. Yazawa, Solid State Ionics 176 (2005) 1145–1149.
[19] Q. Li, Y. Fan, H. Zhao, L.H. Huo, Chin. J. Inorg. Chem. 22 (2006) 2025–2030.
[20] J.F. Gao, X.Q. Liu, D.K. Peng, G.Y. Meng, Catal. Today 82 (2003) 207–211.